ACS MATERIALS Au
AN OPEN ACCESS JOURNAL OF THE AMERICAN CHEMICAL SOCIETY

pubs.acs.org/materialsau Article

# Three-Dimensional Printed $MoS_2$/Graphene Aerogel Electrodes for Hydrogen Evolution Reactions

Swetha Chandrasekaran,*,‡ Jeremy Feaster,‡ Jenna Ynzunza, Frances Li, Xueqiao Wang, Art J. Nelson, and Marcus A. Worsley*

Cite This: *ACS Mater. Au* 2022, 2, 596–601 Read Online

ACCESS | Metrics & More | Article Recommendations | Supporting Information

**ABSTRACT:** In this work, we demonstrate the use of direct ink writing (DIW) technology to create 3D catalytic electrodes for electrochemical applications. Hybrid $MoS_2$/graphene aerogels are made by mixing commercially available $MoS_2$ and graphene oxide powders into a thixotropic, high concentration, viscous ink. A porous 3D structure of 2D graphene sheets and $MoS_2$ particles was created after post treatment by freeze-drying and reducing graphene oxide through annealing. The composition and morphology of the samples were fully characterized through XPS, BET, and SEM/EDS. The resulting 3D printed $MoS_2$/graphene aerogel electrodes had a remarkable electrochemically active surface area (>1700 $cm^2$) and were able to achieve currents over 100 mA in acidic media. Notably, the catalytic activity of the $MoS_2$/graphene aerogel electrodes was maintained with minimal loss in surface area compared to the non-3D printed electrodes, suggesting that DIW can be a viable method of producing durable electrodes with a high surface area for water splitting. This demonstrates that 3D printing a $MoS_2$/graphene 3D porous network directly using our approach not only improves electrolyte dispersion and facilitates catalyst utilization but also provides multidimensional electron transport channels for improving electronic conductivity.

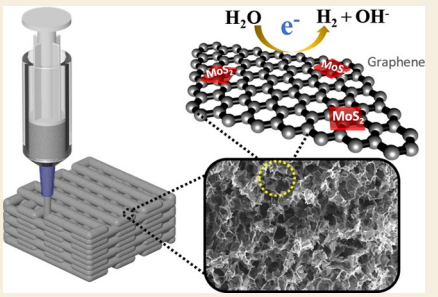


**KEYWORDS:** *3D printing, $MoS_2$, graphene, hydrogen evolution reaction, aerogel, catalysis, additive manufacturing, electrochemistry*

## INTRODUCTION

By 2050, the U.S. Energy Information Administration (EIS) predicts a 50% rise in worldwide energy use.[1] The growing worry about the impact of anthropogenic greenhouse gas (GHG) emissions on the earth's climate drives us to seek out more environmentally friendly and sustainable energy options. With the focus shifting to such systems, storing these sustainable energy sources has received much attention. Through electro-photochemical water splitting, energy storage in the form of hydrogen (a high energy density, carbon free carrier) has been proven to be a potential technique for intermittent energy storage.[2,3] The development of active, stable, low-cost, earth-abundant electrocatalysts is required to make this technology more viable and widespread. The hydrogen evolution reaction (HER), in which two hydrogen ions are reduced to molecular hydrogen, is the main step in electrochemical water splitting. Due to its high activity, electrochemical inertness, and close-to-thermoneutral hydrogen binding energy, platinum (Pt) is the most extremely utilized catalyst for HER to date.[4]

Because of their low cost, great abundance, robustness, and hydrogen production efficiency, layered transition metal dichalcogenides (TMDs) have recently been explored as next-generation electrocatalytic materials.[5,6] For HER, $MoS_2$ is the most promising and well-studied material.[7] The edge sites of $MoS_2$ have been shown to be catalytically active toward HER in both theoretical and experimental studies. However, because of the natural stacking and aggregation of 2D sheets, the number of active sites is reduced, and the poor intrinsic electrical conductivity makes its use as an efficient catalyst difficult.[8,9] To address this, these are often hybridized by adding conductive fillers, especially graphene.[10,11]

A graphene aerogel (GA) is a porous 3D carbon framework of 2D sheets with a high surface area that not only enhances electrolyte flow and facilitates catalyst use but also has a high electrical conductivity.[12−14] GA appears to be a good scaffold for increasing the catalytic activity of supporting materials based on these features. Previous works have shown a straightforward method for using the architecture of a precursor graphene aerogel to generate multilayer dichalcogenide aerogels.[15,16] When compared to graphene precursor aerogels, the hybrid graphene/$MoS_2$ conductive aerogel had a higher surface area and 10 times lower HER current when tested for catalytic activity. Similarly, by using GA as the matrix, Wang *et al.* developed a 3D graphene $MoS_2$ aerogel that

Received: February 7, 2022
Revised: April 24, 2022
Accepted: April 25, 2022
Published: May 5, 2022





https://doi.org/10.1021/acsmaterialsau.2c00014
*ACS Mater. Au* 2022, 2, 596–601

exhibited 6−8 times larger electrochemically active area, resulting in high catalytic performance.[17] Zhang *et al.* reported an effective electrocatalytic activity for HER when graphene oxide (GO) is doped with nitrogen, resulting in a low overpotential of 112 mV.[18]

Traditional methods for designing and fabricating 3D electrocatalytic electrodes either use solution casting, hydrothermal gelation, or electrodeposition.[19,20] The properties of the catalyst are known to be influenced by both its composition and structure. Thus, the construction of 2D nanosheets in a 3D framework may open new possibilities for improving catalyst performance. 3D printing, or additive manufacturing, is a process that allows for the rapid prototyping of both simple and sophisticated 3D objects from a variety of precursor materials. Fused deposition modeling (FDM) with carbon filaments, direct ink writing (DIW) with conductive inks, and selective laser melting (SLM) with metal powders are the most often documented 3D printing technologies for the manufacture of electrodes for electrochemical energy applications.[21,22] SLM uses metal powders (e.g., stainless steel and titanium) and is often modified by electrodeposition to adhere catalysts to the surface.[23] FDM, on the other hand, uses commercial carbon black powders and thermoplastic polymers as precursor materials.[24] Microextrusion of graphene-based inks has been used to illustrate the potential of additive manufacturing to fabricate 3D porous carbons.[25−28]

Extrusion-based direct ink writing[22] (DIW) is a process in which an "ink" is extruded through a nozzle as directed by a computer-controlled stage. 3D structures are produced by finely tuning the ink composition to attain a thixotropic rheological behavior and building multiple layers of materials on the printer substrate. 3D printing aerogels enables one to create structures with both high surface area and fast transport pathways to simultaneously promote interfacial phenomena and species transport for a number of energy-related applications. Often, additives such as polymers and inorganic fillers[29] are used to adjust the ink's rheological qualities. The pH of GO is adjusted after it is mixed with a branched copolymer surfactant to generate a non-covalent network of GO sheets with optimal rheology.[30] Multimaterial graphene- and copper-based aqueous inks were created by forming a colloidal thermoresponsive ink using Pluronic F-127.[31] Biocompatible inks were also created by choosing appropriate modifiers such as cellulose nanofibers,[32−34] polylactide-*co*-glycolide (a biocompatible elastomer),[35] and alginates[36] to 3D print graphene scaffolds. Sol−gel-based printing is also widely used where the ink is partially gelled to reach intersheet attraction and ion cross-linking.[37−39] Binder-less methods have also been used to 3D print GO microlattices, in which a high-concentration GO suspension is generated by evaporation of the solvent or centrifugation.[40,41]

To date, Lin *et al.* alone have published 3D printed $MoS_2$/graphene electrodes. Their study employs a 3D freeze-casting approach that combines inkjet printing with freeze-casting to create a hybrid aerogel comprising small $MoS_2$ patches linked to larger 2D graphene flakes in a macroporous framework as an anode for sodium-ion batteries.[42] In this work, DIW[43] of an ink that combines a highly porous graphene aerogel and commercially available $MoS_2$ powders is used to build a hierarchical 3D framework of the catalyst. Our 3D printed GA/$MoS_2$ electrodes combine the benefits of both GA and $MoS_2$ with 3D printing to create an effective mass flow-controlled electrocatalysts with a high accessible surface area.

## RESULTS AND DISCUSSION

A high concentration, viscous aqueous ink is formulated by combining 4 wt % graphene oxide powders (300−800 nm platelet size) and 4 wt % commercially purchased $MoS_2$ powders. For DIW, the inks must have a shear thinning rheological behavior, i.e., it must flow smoothly under shear (e.g., through the nozzle) while maintaining its shape immediately after deposition. GO/$MoS_2$ ink is prepared by adding appropriate amounts of hydroxy propyl methyl cellulose. A detailed description of ink preparation and 3D printing can be found in the Supporting Information.

The rheological behavior of GO dispersions has recently been studied in order to enable the construction of GO into more complicated designs.[44] Using high concentration (40 mg/mL) aqueous graphene oxide suspensions, Zhu *et al.* showed 3D printing of graphene aerogels suitable for DIW. The elastic modulus and yield stress of the 40 mg/mL suspension were an order of magnitude higher than those of the 20 mg/mL suspension, according to our earlier findings.[25] As a result, a 40 mg/mL GO suspension was utilized for this study. Figure 1b shows the viscosity of the as-prepared GO/

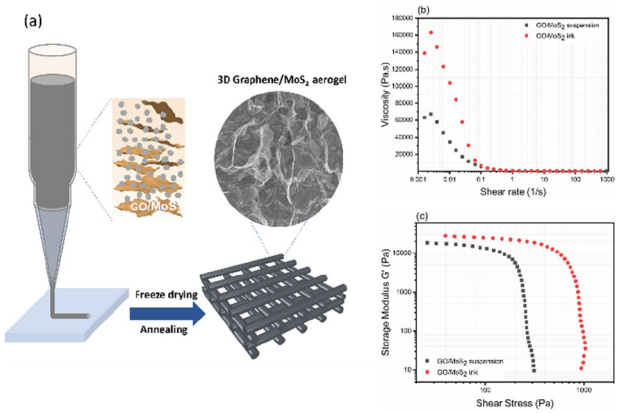


**Figure 1.** (a−c) DIW of GO/$MoS_2$ with rheological studies.

$MoS_2$ suspension and GO/$MoS_2$ ink as a function of shear rate. The ink now has a higher viscosity and the requisite shear thinning behavior due to the addition of cellulose. Although the GO/$MoS_2$ suspension exhibits a similar behavior, without cellulose, it does not have sufficient stiffness (as seen in Figure 1c), evidenced by an inability to hold its shape after deposition. The as-prepared suspension has a plateau value of its elastic modulus $G'$ at 18,000 Pa and a yield stress ($\tau_y$) of 230 Pa. Both the modulus and yield stress increased by 50% and 200%, respectively, when the cellulose viscosifier was added. Cellulose forms a hydrogel in water through physical cross-linking due to the presence of numerous hydroxyl groups, which can form a polymer network through hydrogen bonding. In this case, the hydrogen bonding can be with both GO and water due to the presence of hydroxyl groups.[45] The inclusion of cellulose not only increases viscosity but also adds stiffness to the ink, improving its printability.

After the ink's rheology is properly tuned, it is loaded into a syringe barrel. The ink is then centrifuged to remove trapped air bubbles before being extruded through a micronozzle to create 3D structures, as shown in the schematic in Figure 1a.


https://doi.org/10.1021/acsmaterialsau.2c00014
ACS Mater. Au 2022, 2, 596−601

Cubic lattices with multiple orthogonal layers of parallel cylindrical rods are printed alternatively on a glass substrate. The rods have the same diameter as the nozzle's inner diameter, and the center-to-center rod spacing is kept constant at 0.8 mm. During the print, the *z*-spacing is adjusted to 60% of the nozzle diameter and the number of layers piled on the structure is modified to reach the appropriate electrode thickness. To avoid cracking or drying due to evaporation of water, soon after printing, the 3D printed structures are immersed in liquid nitrogen and freeze-dried for 48 h in vacuum to form aerogels. The printed aerogels are then subjected to a heat treatment process where the samples are annealed in a tube furnace at 1050 °C for 3 h under 4% $H_2$ in an Ar atmosphere. To avoid oxidation of molybdenum during the thermal reduction of graphene oxide, excess sulfur was placed near the inlet of the tube furnace. Both monoliths and simple cubic lattices were printed and processed in this manner. For electrochemical investigations, graphene aerogel monoliths and lattices made with graphene inks (no $MoS_2$) were used as control (reference) samples.[46]

A highly porous network of graphene sheets containing $MoS_2$ particles arrayed in a 3D network can be seen in the cross section of a printed ligament (Figure 2a). The $MoS_2$ particle in the 3D graphene sheet network can be seen at a higher magnification in the micrographs (indicated by the red arrow in Figure 2b). The lower magnification of elemental analysis (Figure 2c-i–iv) clearly demonstrates a homogeneous dispersion of $MoS_2$ particles in a graphene aerogel. The SEM/EDS image of as-received $MoS_2$ powders and the back-scattered electron image of GA/$MoS_2$ are presented in Figure S1 (Supporting Information). The resulting hybrid aerogel, GA/$MoS_2$, contained 10 wt % $MoS_2$ in XPS analysis. The XPS spectrum analysis of the aerogel is shown in Figure S2 (Supporting Information).

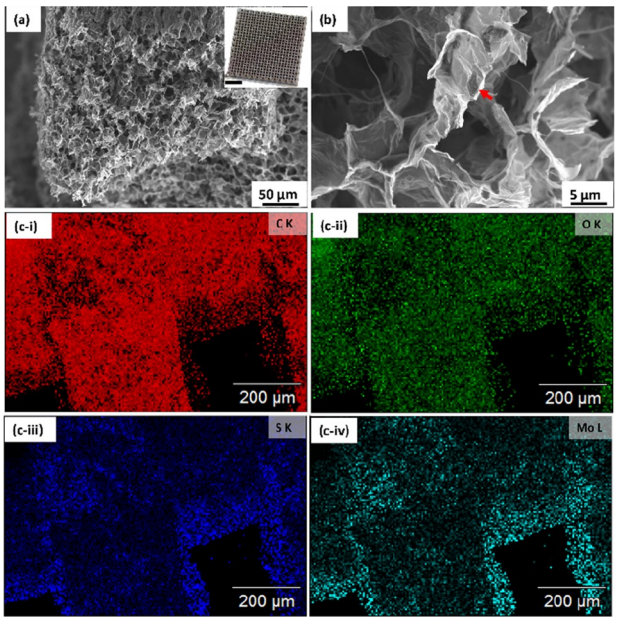


**Figure 2.** (a, b) Scanning electron micrographs of a 3D printed graphene/$MoS_2$ aerogel (inset scale bar: 5 mm) and (c-i–iv) elemental image analysis of the GA/$MoS_2$ aerogel.

The nitrogen adsorption/desorption isotherms for GA/$MoS_2$ aerogels had a type 4 hysteresis loop (IUPAC classification), which is common in mesoporous solids and is characterized by hysteresis between the adsorption and desorption branches. The layer-by-layer adsorption on a highly homogeneous surface is represented by the stepwise isotherm in Figure 3a. The Barrett–Joyner–Halenda (BJH) method is used to determine the pore size distribution in the aerogel. Figure 3b reveals that majority of the volume has a pore size distribution of 1–2 nm.

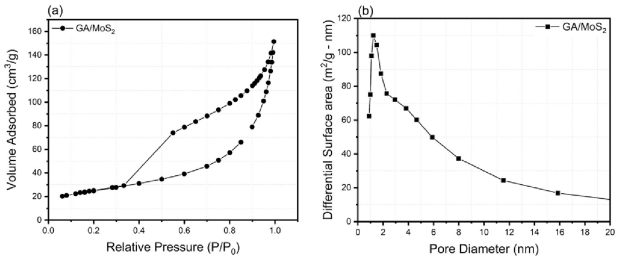


**Figure 3.** (a) Nitrogen adsorption–desorption isotherms and (b) BJH pore size distribution derived from the desorption isotherms of GA/$MoS_2$.

The 3D printed GA/$MoS_2$ monolith and lattice samples have densities of 80 and 64 mg/cm$^3$, respectively. When evaluated by nitrogen porosimetry, these aerogels had a surface area of 89 m$^2$/g. This is greater than the surface area of a graphene aerogel made in a similar manner (26 m$^2$/g). Previous GA/$MoS_2$ aerogels exhibited surface areas of 691m$^2$/g[15] due to the utilization of critical point-dried graphene aerogels with native surface areas up to 1300 m$^2$/g.[12] The GA/$MoS_2$ used in this study was obtained by freeze-drying, resulting in a comparatively lower but still high surface area.

The samples were then evaluated for their electrochemical performance using an experimental setup previously developed by our group.[47] First, to estimate the electrochemically active surface area (ECSA) of each aerogel, cyclic voltammetry (CV) was used to measure the double-layer capacitance in a non-Faradaic potential window (Figure 4a). Four scan rates were

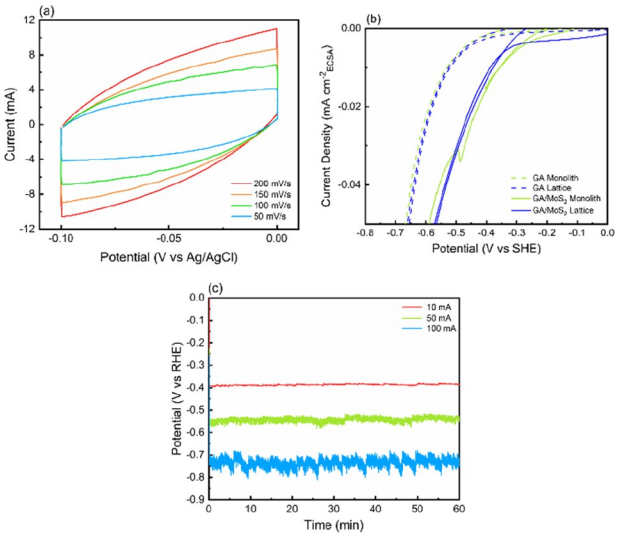


**Figure 4.** Electrochemical results from testing the 3D printed electrodes. (a) ECSA of the 3D printed GA/$MoS_2$ lattice. (b) CV curves of samples on a current density basis. (c) CP of the GA/$MoS_2$ lattice at 10, 50, and 100 mA showing stability over 1 h.


https://doi.org/10.1021/acsmaterialsau.2c00014
ACS Mater. Au 2022, 2, 596–601

used: 200, 150, 100, and 50 mV/s. For the graphene aerogel (i.e., control) lattices and monoliths, the ECSAs were ∼800 and ∼1540 $cm^2$, respectively. These values were based on a geometric surface area of 1.4 $cm^2$ and a reference capacitance of 21 $\mu F/cm^2$ measured on a flat Au foil. As expected, the monoliths had a higher ECSA than the lattices, which had open spacing between the rods. For the GA/$MoS_2$ lattices and monoliths, the ECSAs were ∼1725 and ∼3100 $cm^2$, respectively. The two-fold increase in ECSA for the 3D printed GA/$MoS_2$ structures compared to the graphene-only control structures is consistent with the addition of $MoS_2$ powders in the ink.

To understand the electrocatalytic activity, CV measurements were taken on all four aerogels across a wider range of potentials (Figure 4b). Each sample was tested in 0.5 M sulfuric acid using an iridium oxide on carbon anode and a Nafion cation exchange membrane. For each sample, the current was normalized by the ECSA to investigate the intrinsic activity of the materials. The total current density of the two GA control samples overlapped with one another, indicating that the activity of the GA monoliths and lattices was consistent and the difference in total current was solely due to the higher ECSA of the monoliths. Additionally, the current density of the GA/$MoS_2$ lattices and monoliths was very similar; this demonstrates that the structure of the electrode—whether as a monolith or a lattice—does not change the intrinsic activity of $MoS_2$ for HER. The GA/$MoS_2$ electrodes demonstrated a clear improvement in activity compared to the GA samples, which was expected due to $MoS_2$'s superior catalytic performance.[48,49] Furthermore, the GA/$MoS_2$ aerogels were able to achieve over 100 mA total current in the acidic electrolyte, indicating that these materials can be used for high production rates of $H_2$ from water.

The samples were also tested using chronopotentiometry (CP) to evaluate their activity for HER as a function of time and current. Gaseous products formed on the cathode were quantified using gas chromatography. All the samples demonstrated high selectivity for $H_2$, and no other gaseous products were measured in the 3D printed reactor. Three different currents (10, 50, and 100 mA) were investigated, and each test was conducted over a 1 h time period (Figure 4c). The GA/$MoS_2$ samples demonstrated lower overpotentials for each of the currents tested compared to the GA samples as expected. However, the GA/$MoS_2$ and GA monolith structures experienced a >60% loss in ECSA after the CP experiment; this is due to $H_2$ gas getting trapped inside the pores of the structure. The bubbles block the electrode and prevent the electrolyte from getting to the catalyst, leading to a reduction in ECSA. The lattice structures comparatively lost <2% of their ECSA under the same conditions, indicating that the structure of the lattice allowed for gaseous products to leave the electrode in a way that did not block the surface area that was available to the catalyst. The GA/$MoS_2$ lattice electrodes, with the combination of a high surface area, high HER activity, and good mass transport of products, demonstrate that DIW can be used to produce robust functionalized aerogels that could be used for a variety of applications for energy conversion and catalysis.

## CONCLUSIONS

The direct ink writing method was used to successfully 3D print a hybrid GA/$MoS_2$ aerogel, demonstrating the potential to control the microstructure of hybrid materials in addition to macroscopic designs. The ink is made up of high concentration commercially available $MoS_2$ particles combined with single layer graphene oxide sheets. The $MoS_2$ particle and GO are converted into a hybrid structure consisting of $MoS_2$ particles homogeneously distributed on the surface of a highly porous GA framework after freeze-drying and thermal annealing. These structures contained high surface areas and ECSAs, and the GA/$MoS_2$ samples outperformed the GA samples for HER over a range of currents. Furthermore, the GA/$MoS_2$ lattices lost very little ECSA while operating at high currents, showcasing their ability to maintain access to the surface area through 3D printed control over mass transport.

## ASSOCIATED CONTENT

### Supporting Information

The Supporting Information is available free of charge at https://pubs.acs.org/doi/10.1021/acsmaterialsau.2c00014.

Detailed information on experimental procedures for ink preparation, printing, and carbonization of GA and GA/$MoS_2$ as well as material characterization techniques such as XPS and SEM/EDS analysis (PDF)

## AUTHOR INFORMATION


### Corresponding Authors

**Swetha Chandrasekaran** − *Materials Science Division, Lawrence Livermore National Laboratory, Livermore, California 94550, United States*; Email: chandrasekar2@llnl.gov

**Marcus A. Worsley** − *Materials Science Division, Lawrence Livermore National Laboratory, Livermore, California 94550, United States*; orcid.org/0000-0002-8012-7727; Email: worsley1@llnl.gov

### Authors

**Jeremy Feaster** − *Materials Science Division, Lawrence Livermore National Laboratory, Livermore, California 94550, United States*

**Jenna Ynzunza** − *Materials Science Division, Lawrence Livermore National Laboratory, Livermore, California 94550, United States*

**Frances Li** − *Materials Science Division, Lawrence Livermore National Laboratory, Livermore, California 94550, United States*; orcid.org/0000-0002-0729-6639

**Xueqiao Wang** − *Materials Science Division, Lawrence Livermore National Laboratory, Livermore, California 94550, United States*

**Art J. Nelson** − *Materials Science Division, Lawrence Livermore National Laboratory, Livermore, California 94550, United States*

Complete contact information is available at: https://pubs.acs.org/10.1021/acsmaterialsau.2c00014


### Author Contributions

‡S.C. and J.F. contributed equally. S.C. and J.F. contributed to conceptualization, investigation, visualization, and writing (original draft preparation). J.Y., F.L., X.W., and A.N. contributed to visualization and investigation. M.A.W. participated in conceptualization, funding acquisition, project administration, supervision, and writing (reviewing and editing). All authors have given approval to the final version of the manuscript.



https://doi.org/10.1021/acsmaterialsau.2c00014
ACS Mater. Au 2022, 2, 596−601

## Funding

This work was done under the auspices of the U.S. Department of Energy under Contract DE-AC52-07NA27344.

## Notes

The authors declare no competing financial interest.

## ■ ABBREVIATIONS

| | |
|---|---|
| GA | graphene aerogel |
| GO | graphene oxide |
| $MoS_2$ | molybdenum disulfide |
| DIW | direct ink writing |
| HER | hydrogen evolution reaction |
| CV | cyclic voltammetry |
| CP | chronopotentiometry |
| ECSA | electrochemically active surface area |

## ■ REFERENCES

(1) *EIA projects nearly 50% increase in world energy usage by 2050, led by growth in Asia - Today in Energy - U.S.* Energy Information Administration (EIA) https://www.eia.gov/todayinenergy/detail.php?id=42342 (accessed 2022−01 -25).
(2) Abbasi, T.; Abbasi, S. A. 'Renewable' Hydrogen: Prospects and Challenges. *Renewable and Sustainable Energy Reviews* **2011**, *15*, 3034−3040.
(3) Walter, M. G.; Warren, E. L.; McKone, J. R.; Boettcher, S. W.; Mi, Q.; Santori, E. A.; Lewis, N. S. Solar Water Splitting Cells. *Chem. Rev.* **2010**, *110*, 6446−6473.
(4) Hansen, J. N.; Prats, H.; Toudahl, K. K.; Mørch Secher, N.; Chan, K.; Kibsgaard, J.; Chorkendorff, I. Is There Anything Better than Pt for HER? *ACS Energy Lett.* **2021**, *6*, 1175−1180.
(5) Chia, X.; Pumera, M. Layered Transition Metal Dichalcogenide Electrochemistry: Journey across the Periodic Table. *Chem. Soc. Rev.* **2018**, *47*, 5602−5613.
(6) Eng, A. Y. S.; Ambrosi, A.; Sofer, Z.; Šimek, P.; Pumera, M. Electrochemistry of Transition Metal Dichalcogenides: Strong Dependence on the Metal-to-Chalcogen Composition and Exfoliation Method. *ACS Nano* **2014**, *8*, 12185−12198.
(7) Yang, Y.-Q.; Zhao, C.-X.; Bai, S.-Y.; Wang, C.-P.; Niu, C.-Y. Activating MoS2 Basal Planes for Hydrogen Evolution through the As Doping and Strain. *Phys. Lett. A* **2019**, *383*, 2997−3000.
(8) Voiry, D.; Salehi, M.; Silva, R.; Fujita, T.; Chen, M.; Asefa, T.; Shenoy, V. B.; Eda, G.; Chhowalla, M. Conducting MoS2 Nanosheets as Catalysts for Hydrogen Evolution Reaction. *Nano Lett.* **2013**, *13*, 6222−6227.
(9) Lukowski, M. A.; Daniel, A. S.; Meng, F.; Forticaux, A.; Li, L.; Jin, S. Enhanced Hydrogen Evolution Catalysis from Chemically Exfoliated Metallic MoS2 Nanosheets. *J. Am. Chem. Soc.* **2013**, *135*, 10274−10277.
(10) Levita, G.; Restuccia, P.; Righi, M. C. Graphene and MoS2 Interacting with Water: A Comparison by Ab Initio Calculations. *Carbon* **2016**, *107*, 878−884.
(11) Roy, K.; Padmanabhan, M.; Goswami, S.; Sai, T. P.; Ramalingam, G.; Raghavan, S.; Ghosh, A. Graphene−MoS2 Hybrid Structures for Multifunctional Photoresponsive Memory Devices. *Nature Nanotech* **2013**, *8*, 826−830.
(12) Worsley, M. A.; Olson, T. Y.; Lee, J. R. I.; Willey, T. M.; Nielsen, M. H.; Roberts, S. K.; Pauzauskie, P. J.; Biener, J.; Satcher, J. H., Jr.; Baumann, T. F. High Surface Area, Sp2-Cross-Linked Three-Dimensional Graphene Monoliths. *J. Phys. Chem. Lett.* **2011**, *2*, 921−925.
(13) Worsley, M. A.; Pauzauskie, P. J.; Olson, T. Y.; Biener, J.; Satcher, J. H., Jr.; Baumann, T. F. Synthesis of Graphene Aerogel with High Electrical Conductivity. *J. Am. Chem. Soc.* **2010**, *132*, 14067−14069.
(14) *Self-Assembled Graphene Hydrogel via a One-Step Hydrothermal Process | ACS Nano* DOI: 10.1021/nn101187z (accessed 2022 -01 -25).
(15) Worsley, M. A.; Shin, S. J.; Merrill, M. D.; Lenhardt, J.; Nelson, A. J.; Woo, L. Y.; Gash, A. E.; Baumann, T. F.; Orme, C. A. Ultralow Density, Monolithic WS2, MoS2, and MoS2/Graphene Aerogels. *ACS Nano* **2015**, *9*, 4698−4705.
(16) Long, H.; Harley-Trochimczyk, A.; Pham, T.; Tang, Z.; Shi, T.; Zettl, A.; Carraro, C.; Worsley, M. A.; Maboudian, R. High Surface Area MoS2/Graphene Hybrid Aerogel for Ultrasensitive NO2 Detection. *Adv. Funct. Mater.* **2016**, *26*, 5158−5165.
(17) MoS2 Nanosheets Supported on 3D Graphene Aerogel as a Highly Efficient Catalyst for Hydrogen Evolution - Zhao - 2015 - Chemistry − A European Journal - Wiley Online Library https://chemistry-europe.onlinelibrary.wiley.com/doi/10.1002/chem.201501964 (accessed 2022 -01 -25).
(18) Dong, H.; Liu, C.; Ye, H.; Hu, L.; Fugetsu, B.; Dai, W.; Cao, Y.; Qi, X.; Lu, H.; Zhang, X. Three-Dimensional Nitrogen-Doped Graphene Supported Molybdenum Disulfide Nanoparticles as an Advanced Catalyst for Hydrogen Evolution Reaction. *Sci. Rep.* **2015**, *5*, 17542.
(19) Ambrosi, A.; Pumera, M. Self-Contained Polymer/Metal 3D Printed Electrochemical Platform for Tailored Water Splitting. *Adv. Funct. Mater.* **2018**, *28*, 1700655.
(20) Xu, Y.; Zheng, C.; Wang, S.; Hou, Y. 3D Arrays of Molybdenum Sulphide Nanosheets on Mo Meshes: Efficient Electrocatalysts for Hydrogen Evolution Reaction. *Electrochim. Acta* **2015**, *174*, 653−659.
(21) Browne, M. P.; Redondo, E.; Pumera, M. 3D Printing for Electrochemical Energy Applications. *Chem. Rev.* **2020**, *120*, 2783−2810.
(22) Lewis, J. A. Direct Ink Writing of 3D Functional Materials. *Adv. Funct. Mater.* **2006**, *16*, 2193−2204.
(23) Ambrosi, A.; Pumera, M. Multimaterial 3D-Printed Water Electrolyzer with Earth-Abundant Electrodeposited Catalysts. *ACS Sustainable Chem. Eng.* **2018**, *6*, 16968−16975.
(24) Foster, C. W.; Down, M. P.; Zhang, Y.; Ji, X.; Rowley-Neale, S. J.; Smith, G. C.; Kelly, P. J.; Banks, C. E. 3D Printed Graphene Based Energy Storage Devices. *Sci. Rep.* **2017**, *7*, 42233.
(25) Zhu, C.; Han, T. Y.-J.; Duoss, E. B.; Golobic, A. M.; Kuntz, J. D.; Spadaccini, C. M.; Worsley, M. A. Highly Compressible 3D Periodic Graphene Aerogel Microlattices. *Nat. Commun.* **2015**, *6*, 6962.
(26) Chandrasekaran, S.; Yao, B.; Liu, T.; Xiao, W.; Song, Y.; Qian, F.; Zhu, C.; Duoss, E. B.; Spadaccini, C. M.; Li, Y.; Worsley, M. A. Direct Ink Writing of Organic and Carbon Aerogels. *Mater. Horiz.* **2018**, *5*, 1166−1175.
(27) Zhang, Q.; Zhang, F.; Medarametla, S. P.; Li, H.; Zhou, C.; Lin, D. 3D Printing of Graphene Aerogels. *Small* **2016**, *12*, 1702−1708.
(28) Lin, Y.; Liu, F.; Casano, G.; Bhavsar, R.; Kinloch, I. A.; Derby, B. Pristine Graphene Aerogels by Room-Temperature Freeze Gelation. *Adv. Mater.* **2016**, *28*, 7993−8000.
(29) Yao, B.; Peng, H.; Zhang, H.; Kang, J.; Zhu, C.; Delgado, G.; Byrne, D.; Faulkner, S.; Freyman, M.; Lu, X.; Worsley, M. A.; Lu, J. Q.; Li, Y. Printing Porous Carbon Aerogels for Low Temperature Supercapacitors. *Nano Lett.* **2021**, *21*, 3731−3737.
(30) García-Tuñon, E.; Barg, S.; Franco, J.; Bell, R.; Eslava, S.; D'Elia, E.; Maher, R. C.; Guitian, F.; Saiz, E. Printing in Three Dimensions with Graphene. *Adv. Mater.* **2015**, *27*, 1688−1693.
(31) Rocha, V. G.; García-Tuñón, E.; Botas, C.; Markoulidis, F.; Feilden, E.; D'Elia, E.; Ni, N.; Shaffer, M.; Saiz, E. Multimaterial 3D Printing of Graphene-Based Electrodes for Electrochemical Energy Storage Using Thermoresponsive Inks. *ACS Appl. Mater. Interfaces* **2017**, *9*, 37136−37145.
(32) Jiang, J.; Oguzlu, H.; Jiang, F. 3D Printing of Lightweight, Super-Strong yet Flexible All-Cellulose Structure. *Chem. Eng. J.* **2021**, *405*, 126668.
(33) Yao, C.; Yi, J.; Lai, H.; Shi, G.; Hu, Y.; Chen, Z.; Zhai, J.; Wang, X.; Zhong, L.; Liu, C. Enhancing the Mechanical Performance of

Reduced Graphene Oxide Aerogel with Cellulose Nanofibers. *ChemNanoMat* **2021**, *7*, 950−957.
(34) Li, V. C.-F.; Dunn, C. K.; Zhang, Z.; Deng, Y.; Qi, H. J. Direct Ink Write (DIW) 3D Printed Cellulose Nanocrystal Aerogel Structures. *Sci. Rep.* **2017**, *7*, 8018.
(35) Jakus, A. E.; Secor, E. B.; Rutz, A. L.; Jordan, S. W.; Hersam, M. C.; Shah, R. N. Three-Dimensional Printing of High-Content Graphene Scaffolds for Electronic and Biomedical Applications. *ACS Nano* **2015**, *9*, 4636−4648.
(36) Olmos-Juste, R.; Alonso-Lerma, B.; Pérez-Jiménez, R.; Gabilondo, N.; Eceiza, A. 3D Printed Alginate-Cellulose Nanofibers Based Patches for Local Curcumin Administration. *Carbohydr. Polym.* **2021**, *264*, 118026.
(37) Jiang, Y.; Xu, Z.; Huang, T.; Liu, Y.; Guo, F.; Xi, J.; Gao, W.; Gao, C. Direct 3D Printing of Ultralight Graphene Oxide Aerogel Microlattices. *Adv. Funct. Mater.* **2018**, *28*, 1707024.
(38) Yang, J.; Wang, H.; Zhou, B.; Shen, J.; Zhang, Z.; Du, A. Versatile Direct Writing of Aerogel-Based Sol−Gel Inks. *Langmuir* **2021**, *37*, 2129−2139.
(39) Ge, Y.; Zhang, T.; Zhou, B.; Wang, H.; Zhang, Z.; Shen, J.; Du, A. Nanostructured Resorcinol-Formaldehyde Ink for 3D Direct Writing. *J. Mater. Res.* **2018**, *33*, 2052−2061.
(40) Yeh, C.-N.; Huang, H.; Lim, A. T. O.; Jhang, R.-H.; Chen, C.-H.; Huang, J. Binder-Free Graphene Oxide Doughs. *Nat. Commun.* **2019**, *10*, 422.
(41) Yun, X.; Lu, B.; Xiong, Z.; Jia, B.; Tang, B.; Mao, H.; Zhang, T.; Wang, X. Direct 3D Printing of a Graphene Oxide Hydrogel for Fabrication of a High Areal Specific Capacitance Microsupercapacitor. *RSC Adv.* **2019**, *9*, 29384−29395.
(42) Brown, E.; Yan, P.; Tekik, H.; Elangovan, A.; Wang, J.; Lin, D.; Li, J. 3D Printing of Hybrid MoS2-Graphene Aerogels as Highly Porous Electrode Materials for Sodium Ion Battery Anodes. *Mater. Des.* **2019**, *170*, 107689.
(43) Lewis, J. A.; Gratson, G. M. Direct Writing in Three Dimensions. *Mater. Today* **2004**, *7*, 32−39.
(44) Naficy, S.; Jalili, R.; Aboutalebi, S. H.; Iii, R. A. G.; Konstantinov, K.; Innis, P. C.; Spinks, G. M.; Poulin, P.; Wallace, G. G. Graphene Oxide Dispersions: Tuning Rheology to Enable Fabrication. *Mater. Horiz.* **2014**, *1*, 326−331.
(45) Kabir, S. M. F.; Sikdar, P. P.; Haque, B.; Bhuiyan, M. A. R.; Ali, A.; Islam, M. N. Cellulose-Based Hydrogel Materials: Chemistry, Properties and Their Prospective Applications. *Prog Biomater* **2018**, *7*, 153−174.
(46) Yao, B.; Chandrasekaran, S.; Zhang, J.; Xiao, W.; Qian, F.; Zhu, C.; Duoss, E. B.; Spadaccini, C. M.; Worsley, M. A.; Li, Y. Efficient 3D Printed Pseudocapacitive Electrodes with Ultrahigh MnO2 Loading. *Joule* **2019**, *3*, 459−470.
(47) Corral, D.; Feaster, J. T.; Sobhani, S.; DeOtte, J. R.; Lee, D. U.; Wong, A. A.; Hamilton, J.; Beck, V. A.; Sarkar, A.; Hahn, C.; Jaramillo, T. F.; Baker, S. E.; Duoss, E. B. Advanced Manufacturing for Electrosynthesis of Fuels and Chemicals from CO2. *Energy Environ. Sci.* **2021**, *14*, 3064−3074.
(48) Li, G.; Zhang, D.; Qiao, Q.; Yu, Y.; Peterson, D.; Zafar, A.; Kumar, R.; Curtarolo, S.; Hunte, F.; Shannon, S.; Zhu, Y.; Yang, W.; Cao, L. All The Catalytic Active Sites of MoS2 for Hydrogen Evolution. *J. Am. Chem. Soc.* **2016**, *138*, 16632−16638.
(49) *Identification of Active Edge Sites for Electrochemical H2 Evolution from MoS2 Nanocatalysts* https://www.science.org/doi/10.1126/science.1141483 (accessed 2022 -01 -20), DOI: 10.1126/science.1141483.


https://doi.org/10.1021/acsmaterialsau.2c00014
*ACS Mater. Au* 2022, 2, 596−601